



# Hydrogen-Induced Adsorption of Carbon Monoxide on the Gold Dimer Cation: A Joint Experimental and DFT Investigation

Marin Vojkovic, Driss Rayane, Rodolphe Antoine, Michel Broyer,  
Abdul-Rahman Allouche, Pierre Mignon, Philippe Dugourd

## ► To cite this version:

Marin Vojkovic, Driss Rayane, Rodolphe Antoine, Michel Broyer, Abdul-Rahman Allouche, et al.. Hydrogen-Induced Adsorption of Carbon Monoxide on the Gold Dimer Cation: A Joint Experimental and DFT Investigation. *Journal of Physical Chemistry A*, 2017, 121 (23), pp.4404 - 4411. 10.1021/acs.jpca.7b01564 . hal-01673953

**HAL Id: hal-01673953**

**<https://hal.science/hal-01673953>**

Submitted on 1 Nov 2020

**HAL** is a multi-disciplinary open access archive for the deposit and dissemination of scientific research documents, whether they are published or not. The documents may come from teaching and research institutions in France or abroad, or from public or private research centers.

L'archive ouverte pluridisciplinaire **HAL**, est destinée au dépôt et à la diffusion de documents scientifiques de niveau recherche, publiés ou non, émanant des établissements d'enseignement et de recherche français ou étrangers, des laboratoires publics ou privés.

# Hydrogen-induced adsorption of carbon monoxide on the gold dimer cation. A joint experimental and DFT investigation.

*Marin Vojkovic, Driss Rayane, Rodolphe Antoine, Michel Broyer, Abdul-Rahman Allouche, Pierre Mignon\* and Philippe Dugourd\**

Institut Lumière Matière, UMR 5306, Université Claude Bernard Lyon 1, CNRS, F-69622 Lyon, France. [philippe.dugourd@univ-lyon1.fr](mailto:philippe.dugourd@univ-lyon1.fr) ; [pierre.mignon@univ-lyon1.fr](mailto:pierre.mignon@univ-lyon1.fr)

**ABSTRACT.** It is demonstrated, using tandem mass spectrometry and radio-frequency ion-trap, that the adsorption of a H atom on the gold dimer cation,  $\text{Au}_2\text{H}^+$ , prevents the dissociation of gold dimer cation and allows for adsorption of CO. Reaction kinetics are measured by employing a radio-frequency ion trap, where  $\text{Au}_2^+$  and CO interact for a given reaction time. The effect of a hydrogen atom is evaluated by comparing reaction rate constants measured for  $\text{Au}_2^+$  and  $\text{Au}_2\text{H}^+$ . The theoretical results for adsorption of CO molecules and their reaction characteristics with  $\text{Au}_2^+$  and  $\text{Au}_2\text{H}^+$  are found to agree with the experimental findings. The joint investigations provide insights into hydrogen atom adsorption effects and consequent reaction mechanisms.

## INTRODUCTION

Since the pioneering work of Haruta et al.<sup>1</sup> on the catalytic activity of small gold nanoparticles on metaloxide supports,<sup>2</sup> there have been tremendous reports on the ability of gold nanoparticles to catalyze a wide range of reactions.<sup>3, 4</sup> Ultra-small particles, i.e. clusters of very low diameters ( $\sim 0.5$  nm) were found to be most effective catalysts.<sup>5</sup> Among the reactions, oxidation of CO is considered as a benchmark reaction to evaluate the catalytic activity. Investigations of this type of reactions on small gas phase clusters facilitate elucidating the detailed reaction mechanism of catalytic activity and the influence of various factors including size and shape of the cluster, charge on the cluster, interaction with the supporting material, adsorption of ligands, and doping with other atoms.

Hydride metal complexes recently received much attention due to their specific reactivity and, as a consequence, open the field for important advances in synthesis and catalysis.<sup>6</sup> Several studies both theoretical and experimental have been made so far to study the influence of hydrogen adduct on the reactivity of metal cluster.<sup>6-15</sup> In the case of CO oxidation over supported gold nanoparticles, traces of hydrogen in the reactant mixture significantly alter the catalytic activity. Molecular hydrogen can overcome the inertness of gold cluster cations towards molecular oxygen.<sup>16</sup> It has been shown that hydrogen doping of small gold clusters allows a better CO adsorption<sup>8, 14</sup> and O<sub>2</sub> activation as well as reduction of reaction barrier for CO oxidation.<sup>17</sup> These properties were confirmed for small Ag clusters.<sup>18</sup> Similarly, the pre-adsorption of H<sub>2</sub>O on the Au<sub>2</sub><sup>+</sup> enhances CO and O<sub>2</sub> adsorption.<sup>19</sup> Phala et al.,<sup>14</sup> studied the chemisorption of hydrogen atom on gold clusters using density functional theory. It was found that the H atom prefers bridged type of bonding with two Au-H bonds on the gold clusters.

Theoretical calculations on reaction mechanisms allowed to show that the  $\text{Au}_n\text{H}$  clusters become more catalytically active in comparison to  $\text{Au}_n$  by lowering the activation energy for the two steps of the CO oxidation reaction.<sup>20</sup>

As such the effect of adsorbed hydrogen atom on small metal clusters appears to be tremendous for catalytic reactivity. Herein we report reaction kinetics measurements using radio-frequency (RF) ion-trap mass-spectrometry combined with first-principles theoretical calculations, on the simplest gold cluster  $\text{Au}_2$  and  $\text{Au}_2\text{H}$  cations, in order to understand reactivity properties.

## EXPERIMENTAL

Figure 1 shows a scheme of the experimental setup. The metal species are synthesized using the LAVESI method,<sup>21</sup> coupling laser vaporization with ESI, and then transferred to the quadrupole ion trap for reactions and detection. The LAVESI experimental setup, designed for synthesis of ligated metal complexes, has been described in detail in previous work.<sup>21</sup> In short, it consists of an LTQ XL mass spectrometer produced by Thermo Fischer Scientific (San Jose, CA, USA). A metal rod is placed in the ESI source of the instrument and irradiated by a nanosecond laser beam. The  $\text{Au}_2^+$  and  $\text{Au}_2\text{H}^+$  species are created in the regime where no ligand is sprayed and only the ESI voltage is applied to help ionize and transfer the species to the ion optics part of the instrument. The gas phase reactions were carried out in the ion trap of the mass spectrometer. Similar setups for gas phase reactions already exist, including modified LTQ mass spectrometers for performing reactions of species obtained in solution synthesis.<sup>22</sup> The reactant was introduced directly into the trap by connecting a bottle of CO seeded helium gas (Air Liquide, Bagneux, France) to the buffer gas tube. By this way, we are able to switch between pure helium and CO

seeded helium. For this experiment, two bottles of CO were used, 5% and 0.1% (v/v) concentrations. Helium gas is pumped with higher efficiency than CO,<sup>23</sup> which is pumped at ~77% of the rate of helium which means that the concentrations of reactants in the ion trap are 6.8% and 0.13% (v/v) when the bottle with 5% and 0.1% mixture respectively are in use.

Upon opening the valve to introduce the gas mixture in the ion trap, a period of ~20 minutes was required for the reactants to diffuse completely through the gas tubes and into the ion trap. Similarly, after the desired experiments with reactants were done, a period of around 20-30 minutes was required for the pure helium gas to flush the reactants completely out of the trap.

### **Computational Details**

In order to assess the adequate theoretical method to describe  $\text{Au}_2^+$  and  $\text{Au}_2\text{H}^+$  complexes, preliminary calculations were carried out on the  $\text{Au}_2\text{H}^+$  species with various DFT methods and basis sets. Geometrical parameters were directly compared with those obtained at the LCCSD(T0) level with the SARC-TZVPP basis sets including relativistic correction which has been tested to give the best geometric parameters and vibrational frequency for the Au-H species in comparison with experiments.<sup>24</sup> Our calculations showed that conventional hybrid (B3LYP) as well as long range corrected functionals (wB97x, M062X, camB3LYP) did not perform well for reproducing the geometrical parameters of the  $\text{Au}_2\text{H}^+$  species. Although PBE seems to perform well for geometric parameters of  $\text{Au}_2\text{H}^+$  species it gives rather poor results for  $\text{Au}^+$  coordinated by CO, see Table S1b. The double hybrid B2PLYP functional, including 53% of Hartree-Fock exchange and 27% of MP2 correlation<sup>25</sup>, instead gave reliable results even with including resolution identification approximation for the MP2 integrals as well as for the Coulomb ones plus a numerical integration for the HF Exchange (results shown in Table S1a-b of the SI). As

such this last method was used for the geometry optimizations with CO molecules. The def2 triple  $\zeta$  plus polarization basis sets were used for the second row elements and the corresponding Stuttgart-Dresden effective core potential basis sets for Au (60 core electrons are replaced by the potential). The geometry optimization was thus performed by including the resolution identification approximations via the ORCA program<sup>26</sup>. For energy and thermodynamic quantities calculations, single points were carried out at the B2PLYP/def2-TZVPP level without applying any approximations. These latter's were performed at 298.15 K with the Gaussian program<sup>27</sup>. The free energies changes are computed according to the free energy of the isolated corresponding  $\text{Au}_2^+$  or  $\text{Au}_2\text{H}^+$  complexes and CO molecules. Various conformers were searched for each complex, only the most relevant and lower in energy complexes are discussed in the present study. A conformer search procedure was carried out for  $\text{Au}_2^+$  or  $\text{Au}_2\text{H}^+$  complexes with one and two CO molecules, consisting in 10 ps molecular dynamics at the semi-empirical PM7 level for which 1000 geometries were selected and the optimized at the DFT level. It was observed that CO never bridged Au atoms in any complex, as could be expected according to its coordination via its electronic doublets.

Dissociation mechanisms were modelled by scanning the Au-Au bond elongation from the equilibrium geometry until a distance of 5 Å with a step size of about 0.05 Å. All geometrical parameters were optimized at each step except the Au-Au bond. This procedure allows us to compute the electronic distribution for the complexes after the Au-Au bond cleavage and thus to predict the charge of the isolated species. The energies of each isolated species are then computed according to this charge distribution. During this procedure no transition states has been observed. Atomic charges and bond orders are obtained from a Mulliken population analysis. It has to be noticed that for  $\text{Au}_2(\text{CO})_n^+$  complexes calculations were performed in spin-

unrestricted formalism since these are open shell systems; only very small spin contamination was observed (see S2 table).

## RESULTS

*Experimental measurements.*  $\text{Au}_2^+$  and  $\text{Au}_2\text{H}^+$  species were produced. By doing tandem MS on both species with narrow mass selection window ( $\Delta m \leq 1\text{Da}$ ), we were able to distinguish the reactivity of  $\text{Au}_2^+$  and  $\text{Au}_2\text{H}^+$ , as shown in Figure 2. Both species are stable in the presence of pure buffer gas, and there is no evidence of bonding of water molecules or oxidation in the mass spectrum. After introducing the CO in the trap, the gold dimer becomes unstable and dissociates when reacting with CO. The products observed are  $\text{Au}(\text{CO})^+$ ,  $\text{Au}(\text{CO})_2^+$ . The reaction kinetics show that the  $\text{Au}(\text{CO})^+$  is formed on a time scale faster than 0.1ms. The onset of  $\text{Au}(\text{CO})_2^+$  comes after 10 ms trapping time, and it increases while the abundance of  $\text{Au}(\text{CO})^+$  decreases indicating that the bigger complex is formed from the smaller one by addition of a CO molecule. The complexes with more CO remain low in intensity even at longer trapping times, and only slight indications of these species can be detected in the mass spectrum. It was shown that  $\text{Au}_2^+$  in reaction with trace amounts of CO at 70 K in the ion trap lead to the observation of  $\text{Au}_2(\text{CO})^+$  as well as  $\text{Au}_2(\text{CO})_3^+$ .<sup>28</sup> Kinetics measurements for  $\text{Au}_2^+$  with CO reaction were also performed at room temperature. Terasaki and coworkers<sup>19</sup> observed that  $\text{Au}_2^+$  adsorbs CO followed by cleavage of Au–Au bond. The amounts of  $\text{Au}(\text{CO})^+$  and  $\text{Au}(\text{CO})_2^+$  produced by the reaction of  $\text{Au}_2^+$  with CO under multiple collision conditions as a function of storage time were reported.<sup>19</sup> Our results are in agreement with this previous work.

Unlike  $\text{Au}_2^+$ , the  $\text{Au}_2\text{H}^+$  doesn't dissociate during reactions with CO. New species are formed by addition of CO on the precursor complex. They correspond to the generic formula,

$\text{Au}_2\text{H}(\text{CO})_n^+$ , where  $n=1,2$ . The hydrogen atom seems to stabilize the complex and prevent dissociation. Furthermore, the  $\text{Au}_2\text{H}^+$  species show lower reactivity than  $\text{Au}_2^+/\text{Au}^+$ . Figure 3 shows the reaction rates for  $\text{Au}_2\text{H}^+$ . It takes trapping times of more than 50 ms to observe some increase in abundance of the CO complexes and the relative intensity of the products remains low even at trapping times longer than 1s, at both high and low CO concentrations. From the reaction rates in Figure 3, the reaction constants ( $k$ ) were calculated (Table 1) by normalizing the reaction rate obtained from the slope of plots by the number of CO molecules per  $\text{cm}^3$ . The helium pressure in the LTQ trap given by the constructor is  $P_{\text{LTQ}}=1$  mTorr (0.133 Pa). The CO pressure is  $P_{\text{LTQ}} \cdot \% \text{CO}$  and is equal to  $9 \cdot 10^{-3}$  Pa (for 5% of CO, e.g. 6.8 % concentration (v/v)). The volumic concentration of CO is given by  $n_{\text{VCO}} = P_{\text{LTQ}} \cdot \% \text{CO} / k_{\text{B}}T$ ,  $k_{\text{B}}$  Boltzmann constant and  $T=300$  K, i.e.  $2.2 \cdot 10^{12} \text{ cm}^{-3}$ . The  $k$  values found depend only slightly on the pressure (from 0.1% to 5%), and perhaps saturation effects occur for 5% of CO. The  $k$  values are 2 to 5 times higher than the published values by Terasaki,<sup>19</sup> which is attributed to uncertainty on the total pressure in ion traps.

*Theoretical observations.* The coordination of the gold dimers  $\text{Au}_2^+$  and  $\text{Au}_2\text{H}^+$  complexes by CO has been tackled through DFT calculations in order to understand the difference between the complexes leading the former to dissociation in contrast to the latter. In the  $\text{Au}_2^+$  dimer cation, the two gold atoms are separated by a distance of 2.438 Å (see Table 2), somehow smaller than for the neutral gold dimer (2.507 Å); the electron has been withdrawn from a d-antibonding molecular orbital (all structures are shown in the SI). The bond between the gold atoms is mainly of  $\sigma$  type with some  $\pi$  contributions, the Mayer bond order being 1.54 a.u. One has to notice that the  $\text{Au}_2^+$  dimer is an open shell system, the spin density being equally shared by the two atoms. One can see that CO coordination stabilizes the system, at least until the third CO (see Figure 4).



CO may coordinate  $\text{Au}_2^+$  through one Au atom leading to a linear molecule or may bridge the two Au atoms. The linear conformation is more favorable energetically by about 0.7 eV, see Table 2. Although the Au-Au distance does not increase much, to 2.611 Å, the bond order decreases by a factor two until 0.76 a.u.. In contrast for the bridged conformation the inter-gold distance increases to 2.990 Å. Dissociation of those complexes would lead to the neutral Au atom and  $\text{Au-CO}^+$  cation with a negative relative free energy at -0.12 eV, which is thus exothermic. The coordination of a second CO may lead to three conformations: one linear, one with a doubly coordinated Au atom and a bridged one; showing the following relative free energies:  $\Delta G = -2.23, -2.15$  and  $-2.11$  eV, respectively. For the linear conformation, the bond length did not increase much however the bond order lowers to 0.46 a.u. For the two latter conformations the Au-Au bond length increased to 2.829 and 2.932 Å, respectively, showing that the Au dimer is almost cleaved. The dissociation would lead to the Au atom and the  $\text{Au(CO)}_2^+$  cation costing only a small amount of free energy:  $\Delta\Delta G \sim 0.2$  eV. The dissociation of the linear conformation to AuCO and  $\text{AuCO}^+$  species is more endothermic. However since the linear conformation shows almost the same relative free energy as the other ones, the crossing from one to another is relatively easy and the dissociation is facilitated as well. For the three CO coordinated complexes the two possible conformations, a bridged and T-shaped one, show close relative free energies  $\Delta G = -3.02$  and  $-2.99$  eV, respectively. From those the dissociation to AuCO and  $\text{Au(CO)}_2^+$  would cost almost as much as the loss of a CO. From the T-shaped conformation the fourth CO coordination would allow a small stabilization of a few eV, but further CO coordination would cost energetically. From the bridged conformation a fourth CO coordination is not feasible, indeed forced coordination leads to another Au-CO cleavage.

The  $\text{Au}_2\text{H}^+$  complex is a closed shell system as compared to the gold cation dimer. In the lowest energy conformation gold atoms are distant by 2.616 Å and bridged by a H atom, thus each gold is involved in a covalent bonding with the other gold atom and with the H ( $d(\text{Au-H})=1.692$  Å), see Table 3 and Figure 5. A small amount of negative charge is present on the H atom (-0.16 a.u.) while the gold are both positively charged (+0.58 a.u.) showing only a small attractive electrostatic interaction between the H and the gold atoms. Here the hydrogen atom accepts electron density from the gold dimer by forming covalent bonds with them and thus stabilizing the system, as shown from the bond orders Au-Au: 0.55a.u. and Au-H 0.59a.u.. As a result the bond between gold atoms is weaker but they are kept together by relatively strong Au-H bonds. CO coordination as shown in figure 5 allows a gain in free energy until the second CO coordination. CO coordinations to gold atoms are comparable ( $d(\text{Au-C}) \leq 2.0$  Å) and the distance between the gold atoms does almost not change ( $d(\text{Au-Au})=2.663$  Å for 1 CO and 2.737 Å for two CO). Dissociation of these complexes in  $\text{AuH} + \text{AuCO}^+$  or  $\text{AuHCO} + \text{AuCO}^+$  would cost a significant amount of free energy:  $\Delta\Delta G \sim 2.1\text{eV}$ ,  $\Delta\Delta G \sim 2.8\text{eV}$  from  $\text{Au}_2\text{HCO}^+$  and  $\text{Au}_2\text{H}(\text{CO})_2^+$ , respectively. As such these dissociation processes are clearly unfavorable. The third CO coordination is somehow weaker ( $d(\text{Au-C}) \geq 2.1$  Å) and leads to a small Au-Au bond opening ( $d(\text{Au-Au})=2.802$  Å), the bond order only lowers until 0.30 a.u.. From this latter, dissociation to  $\text{AuHCO} + \text{Au}(\text{CO})_2^+$  is less unfavorable  $\Delta\Delta G \sim 0.6\text{eV}$ , although the loss of a CO or the coordination to a fourth CO are easier possibilities. From a free energy point of view, further CO coordinations are comparable to this one. It has to be noticed that a fourth CO coordination to the  $\text{Au}_2\text{H}(\text{CO})_3^+$  complex is not possible but rather leads to a weak coordination through Van der Waals bonding. For each  $\text{Au}_2\text{H}(\text{CO})_n^+$  complex with  $n=3,4,5$  the dissociation of  $\text{Au}_2\text{H}$  is always the most unfavorable pathway as to the weak coordination of a new CO.  $\Delta\Delta G$  for dissociation

are +0.71 eV, +0.56 eV and +0.48 eV while  $\Delta\Delta G$  for weak coordination are +0.28 eV, +0.17 eV and +0.38 eV, respectively to  $n \times \text{CO} = 3, 4, 5$ . Indeed, energetically the complexes would rather either lose a CO or coordinate a new CO than dissociate. For the complexes with 6 or 7 CO, we see that the last two coordinated CO are only weakly bonded and interact only through van der Waals interactions, the Au-C distances being around 4.2 Å.

## DISCUSSION

Theoretical results allow explaining the fact that  $\text{Au}_2^+$  dissociates and  $\text{Au}_2\text{H}^+$  does not. In fact, the  $\text{Au}_2^+$  dissociation appears rather as an expected process: upon CO coordination to gold atoms, the Au-Au bond becomes weaker and gets broken. From kinetics (see figure 3) it appears that the  $\text{Au}_2^+$  dissociates much faster than  $\text{Au}_2\text{H}^+$  “reacts” with CO. This may be due to the fact that  $\text{Au}_2^+$  is a radical and associates rapidly with CO, and moreover it can directly dissociate to give  $\text{AuCO}^+$ . Although the free energy gain is relatively weak the reaction is exothermic.  $\text{Au}(\text{CO})_2^+$ , which is observed may be formed from the CO coordination to  $\text{AuCO}^+$  or from the coordination of a second CO yielding  $\text{Au}_2(\text{CO})_2^+$  which can dissociate easily and bring  $\text{Au}(\text{CO})_2^+$ . Experimental results showed that the  $\text{AuCO}^+$  complex is formed prior to  $\text{Au}(\text{CO})_2^+$  suggesting that the latter complex is formed from the former and thus validates the first scenario.

For  $\text{Au}_2\text{H}^+$ , the results are more surprising. Indeed, this complex appears to be much more solid and difficult to cleave as the presence of the hydrogen atom allows the gold atoms to form strong covalent bonds with H, evidenced by a charge transfer from gold atoms to H. We observe that the coordination of CO stabilizes the system from an energetic point of view until two CO. This is in very good agreement with the MS spectra where a small peak appears for  $\text{Au}_2\text{HCO}^+$  and a well-defined peak is observed for  $\text{Au}_2\text{H}(\text{CO})_2^+$ . Further CO coordinations are less easy as

seen from the free energy diagram (figure 5) but still possible. Only small peaks are observed for 6 CO coordinated complexes in the MS spectra of figure 2.

The effect of the hydrogen atom in the  $\text{Au}_2\text{H}^+$  complex is quite striking. Indeed it prevents the dissociation of gold dimer and allows anchoring of CO molecules which is a first step toward reactivity. The effect of H mainly consists in strengthening indirectly the cohesion between the two gold atoms. Indeed, although the Au-Au bond is not very strong, the covalent Au-H bonds (Au-H bond order equals 0.59 a.u.) results in a rather solid three body complex. Beyond stabilization of the gold dimer cation, formation of a  $\text{Au}_2\text{H}$  motif might have important consequences on catalytic properties of small clusters. Indeed, the effect of pre-adsorption of H on Au nanoparticle made of 6 or 8 gold atoms has been shown to facilitate the CO oxidation<sup>20</sup>. It was shown that the presence of H enhances the binding of  $\text{O}_2$  molecules to gold and lowers reaction barriers for C-O bond formation or breaking, the effect of the better binding being around 1eV while the effect on reaction barriers is around 0.3 eV. This was also observed for silver nano-clusters.<sup>18</sup> From the results we obtain from the present work, we see that the effect of H is to enhance the covalent bonding between the two bridging Au atoms. Thus on a symmetric  $\text{Au}_6$  or  $\text{Au}_8$  cluster, the effect of a bridging hydrogen atom is to strengthen one Au-Au bond and as a result weaken the remaining bonds with surrounding Au atoms. The symmetry is then broken and it provides reactive sites as compared to a symmetrical cluster in the absence of bridging hydrogen that would be more inert. This is also in good agreement with the observation of Terasaki et al.<sup>19</sup> who observed that the pre-adsorption of a water molecule on a gold dimer cation enhances the  $\text{O}_2$  adsorption allowing thus CO oxidation. This also leads to a strong three body complex and results in more reactive surrounding Au atoms.

## CONCLUSION

We have presented reaction kinetics of  $\text{Au}_2^+$  and  $\text{Au}_2\text{H}^+$  with CO molecules.  $\text{Au}_2^+$  was found to rapidly react to CO coordination leading to a dissociation of the  $\text{Au}_2^+$  dimer. Adsorption of H atom on  $\text{Au}_2^+$  leads to CO adsorption and prevents the Au–Au bond cleavage. In parallel, DFT calculations shed light on the effect of doping a single hydrogen atom in  $\text{Au}_2^+$  on the adsorption of CO molecules. The effect of H mainly consists in strengthening the atomic cohesion through relatively strong Au-H covalent bonds. Beyond stabilization of the gold dimer cation, formation of a  $\text{Au}_2\text{H}$  motif might have important consequences on catalytic properties of small clusters.

#### **ACKNOWLEDGMENT.**

Jin Chenhao and Li Shouchao are acknowledged for the very good work in calibrating DFT methods to reproduce geometrical parameters, preliminary work in computational details and SI. Acknowledgment is also addressed to computing centres: GENCI (project x2016087662) and Pôle Scientifique de Modélisation Numérique (PSMN).

**Table 1.** Reaction constants for the  $\text{Au}_2^+$  dissociation and  $\text{Au}_2\text{H}^+$  reactions with CO.

	CO(0.1%)	CO(5%)
$k(\text{Au}_2^+ + \text{CO} \rightarrow \text{Au}(\text{CO})^+ + \text{Au})$ [cm <sup>3</sup> /s]	$5.5 \cdot 10^{-12}$	$2.5 \cdot 10^{-12}$
$k(\text{Au}_2\text{H}^+ + \text{CO} \rightarrow \text{Au}_2\text{H}(\text{CO})^+) \text{ [cm}^3/\text{s]}$	$1.3 \cdot 10^{-12}$	$4.4 \cdot 10^{-13}$

**Table 2.** Au<sub>2</sub><sup>+</sup> complexes free energy changes computed from the isolated species Au<sub>2</sub><sup>+</sup> and N×(CO) in eV, inter-atomic distances in Å and Au-Au bond orders in a.u.. Corresponding linear and bridge structures and energy diagram are shown in figure 4. Values in parentheses correspond to the two CO coordinating the same Au atom in an orthogonal conformation (see figure 4).

N×(CO)		0	1	2	3	4	5	6
linear	ΔG	0,00	-1,57	-2,23 (-2,15)	-2,99	-3,11	-2,59	-2,39
	d(Au-Au)	2,438	2,611	2,694 (2,829)	2,629	2,873	2,938	3,070
	d(Au-CO)		1,951	2,002 (2,015)	1,985/1,991	1,989	2,009/2,016/ 2,037/2,052/ 2,133	2,044
	b.o. (Au-Au)	1.54	0.25	0.46 (0.32)	0.36	0.41	0.37	0.29
bridge	ΔG		-0,84	-2,11	-3,02	-2,88		
	d(Au-Au)		2,990	2,932	3,385	3,322		
	d(Au-CO)		2,002	2,071/2,059/ 2,031	1,983/2,071	1,988/1,992/ 2,061/2,070/ 3,176		
	b.o. (Au-Au)		0.25	0.16	<0.1	<0.1		

**Table 3.** Au<sub>2</sub>H<sup>+</sup> complexes free energy changes computed from the isolated species Au<sub>2</sub>H<sup>+</sup> and N×(CO) in eV, inter-atomic distances in Å and Au-Au bond orders in a.u.. Corresponding structures and an energy diagram are shown in Figure 5.

N×(CO)	0	1	2	3	4	5	6	7
ΔG	0,00	-1,38	-2,75	-2,60	-2,32	-2,15	-1,77	-1,57
d(Au-Au)	2,616	2,663	2,737	2,802	2,781	2,821	2,797	2,792
d(Au-H)	1,692	1,626/1,794	1,706	1,693/1,778	1,711/1,755	1,679/1,802	1,692/1,792	1,689/1,802
d(Au-CO)		1,980	1,972	1,985/2,015/ 2,113	1,985/2,024/ 2,122/3,152	1,985/2,007/ 2,103/2,940/ 3,666	1,996/2,023/ 2,080/3,147/ 3,467/4,202	1,991/2,025/ 2,073/3,044/ 3,267/3,506/ 4,313
b.o. (Au-Au)	0.56	0.46	0.35	0.29	0.36	0.32	0.36	0.35



**Figure 1.** Scheme of the experimental setup. The LAVESI source is used to vaporize the gold rod. Aided by the ESI voltage, the species are transferred to the entrance flange and guided by the ion optics to the quadrupole ion trap where  $\text{Au}_2^+$  and  $\text{Au}_2\text{H}^+$  species are isolated and trapped for different time intervals to react with CO, which is introduced through the Helium buffer gas line.

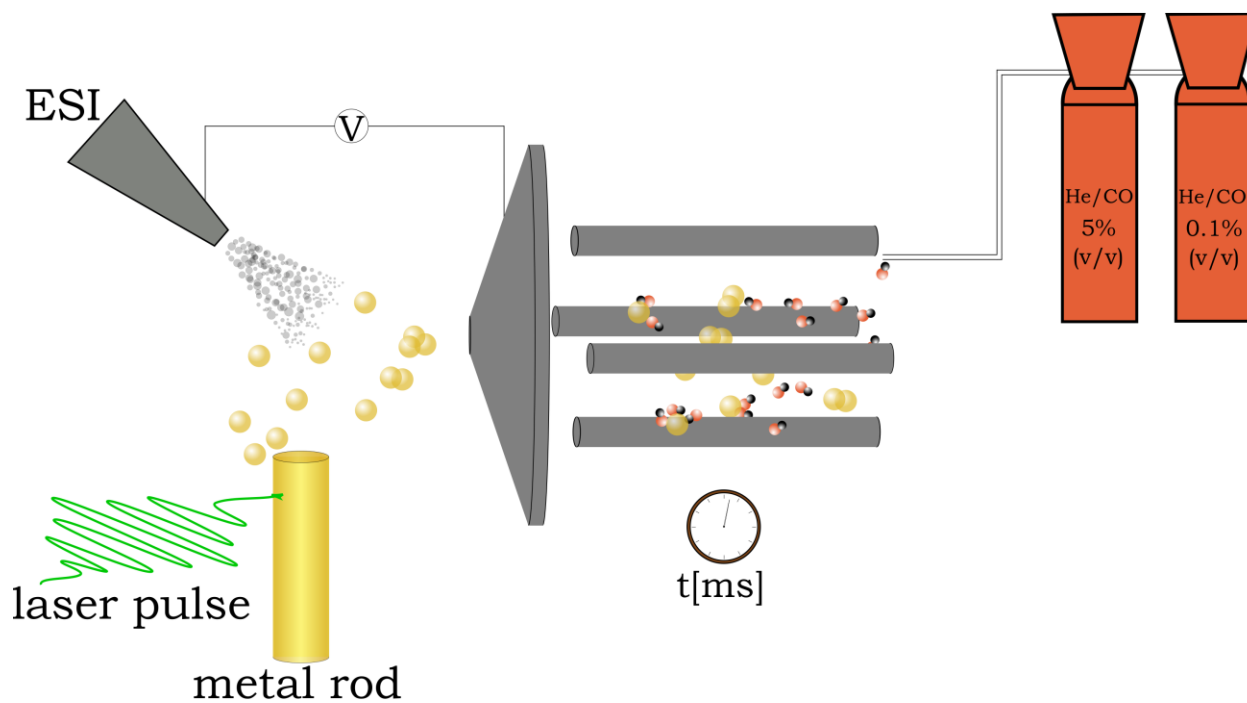


**Figure 2.** Normalized MS2 spectra of the  $\text{Au}_2^+$  (a-b) and  $\text{Au}_2\text{H}^+$  (c-d) species in pure He buffer gas (a and c) and in 5% (v/v) CO seeded helium (b and d). The peak labelled by # is due to a mixing of  $\text{Au}_2\text{H}_2(\text{CO})_6^+$  and  $\text{Au}_2\text{H}_3(\text{CO})_6^+$ .

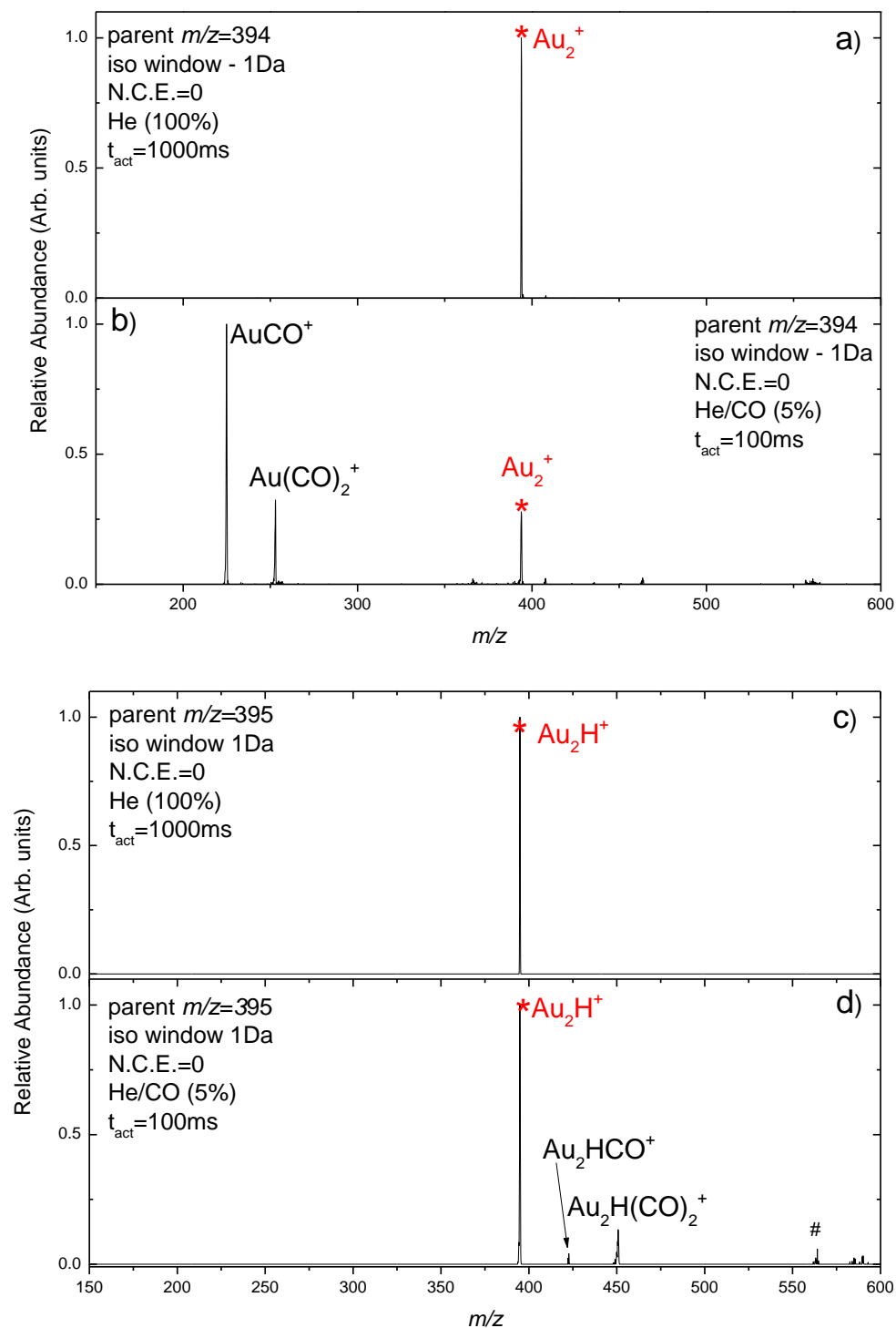


**Figure 3.** Reaction rates for (top) the dissociation of  $\text{Au}_2^+$  ( $\text{Au}_2^+ + \text{CO} \rightarrow \text{Au}(\text{CO})^+ + \text{Au}$ ) and (bottom) reaction of  $\text{Au}_2\text{H}^+$  ( $\text{Au}_2\text{H}^+ + \text{CO} \rightarrow \text{Au}_2\text{H}(\text{CO})^+$ ) in two different CO concentrations (0.1% and 5%). Slopes of linear fits for each reaction are:  $-5.43 \text{ s}^{-1}$  and  $-0.23 \text{ s}^{-1}$  for the dissociation of  $\text{Au}_2^+$  for high and low concentration respectively;  $-0.97 \text{ s}^{-1}$  and  $-0.054 \text{ s}^{-1}$  for the reaction of  $\text{Au}_2\text{H}^+$  for high and low concentration respectively.

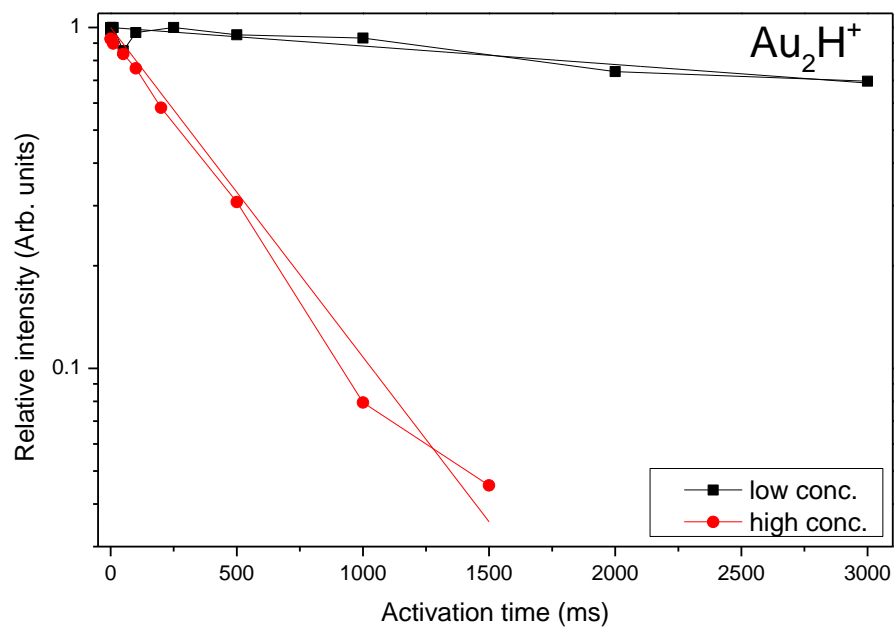
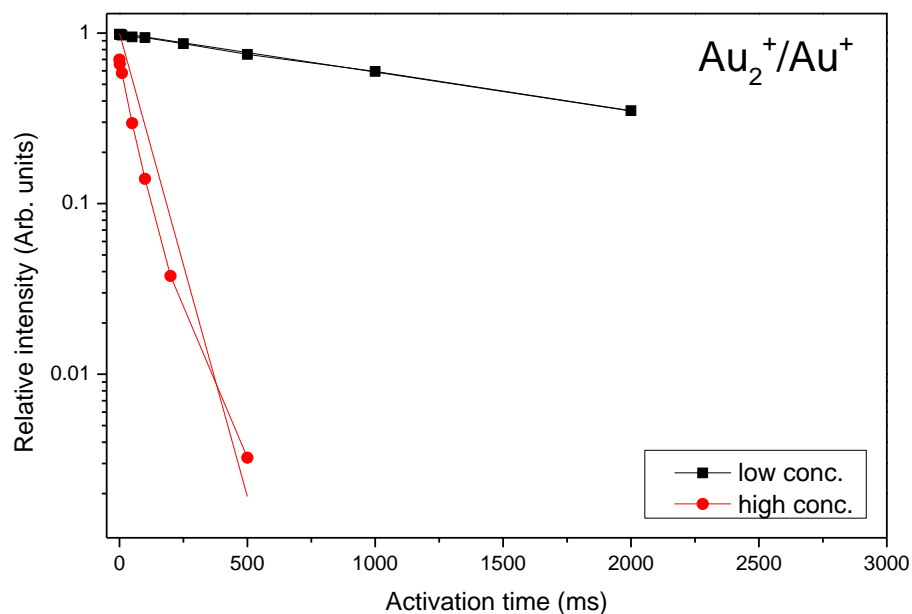


**Figure 4.** Free energy diagram (in eV) of the  $\text{Au}_2^+$  complex as a function of the number of coordinating CO. The blue points correspond to coordinated complexes. Green points correspond to dissociated species. The free energies of the dissociated complexes:  $\text{Au} + \text{AuCO}^+$  for one coordinated CO and for two coordinated CO:  $\text{Au} + \text{Au}(\text{CO})_2^+$  and  $\text{AuCO} + \text{AuCO}^+$  are:  $\Delta G = -0.12$  eV,  $-1.93$  eV and  $-0.31$  eV, respectively. Dissociations from one or two CO coordinated complexes leading to  $\text{Au}^+ + \text{AuCO}$  or  $\text{Au}^+ + \text{Au}(\text{CO})_2$  (not shown) correspond to  $\Delta G = +1.40$  eV and  $+3.34$  eV, respectively.

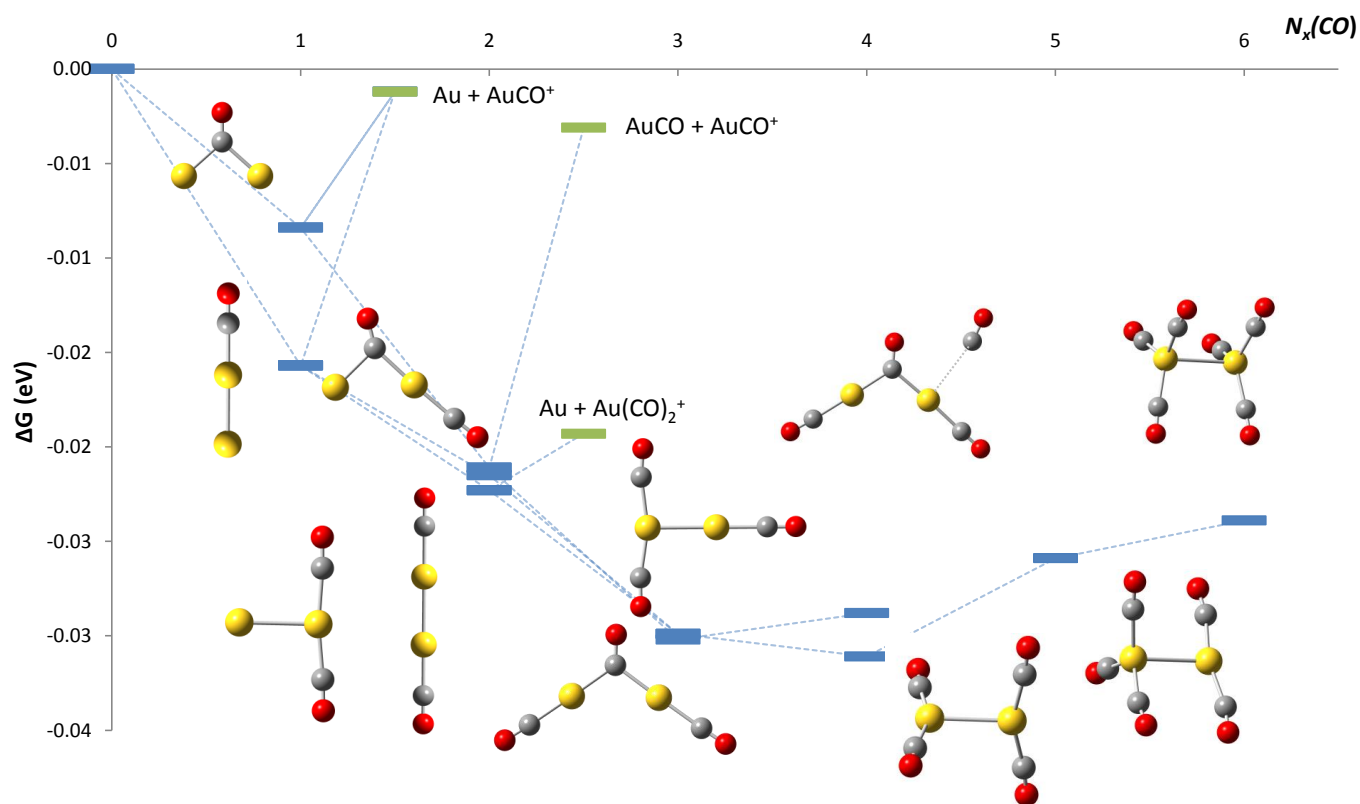
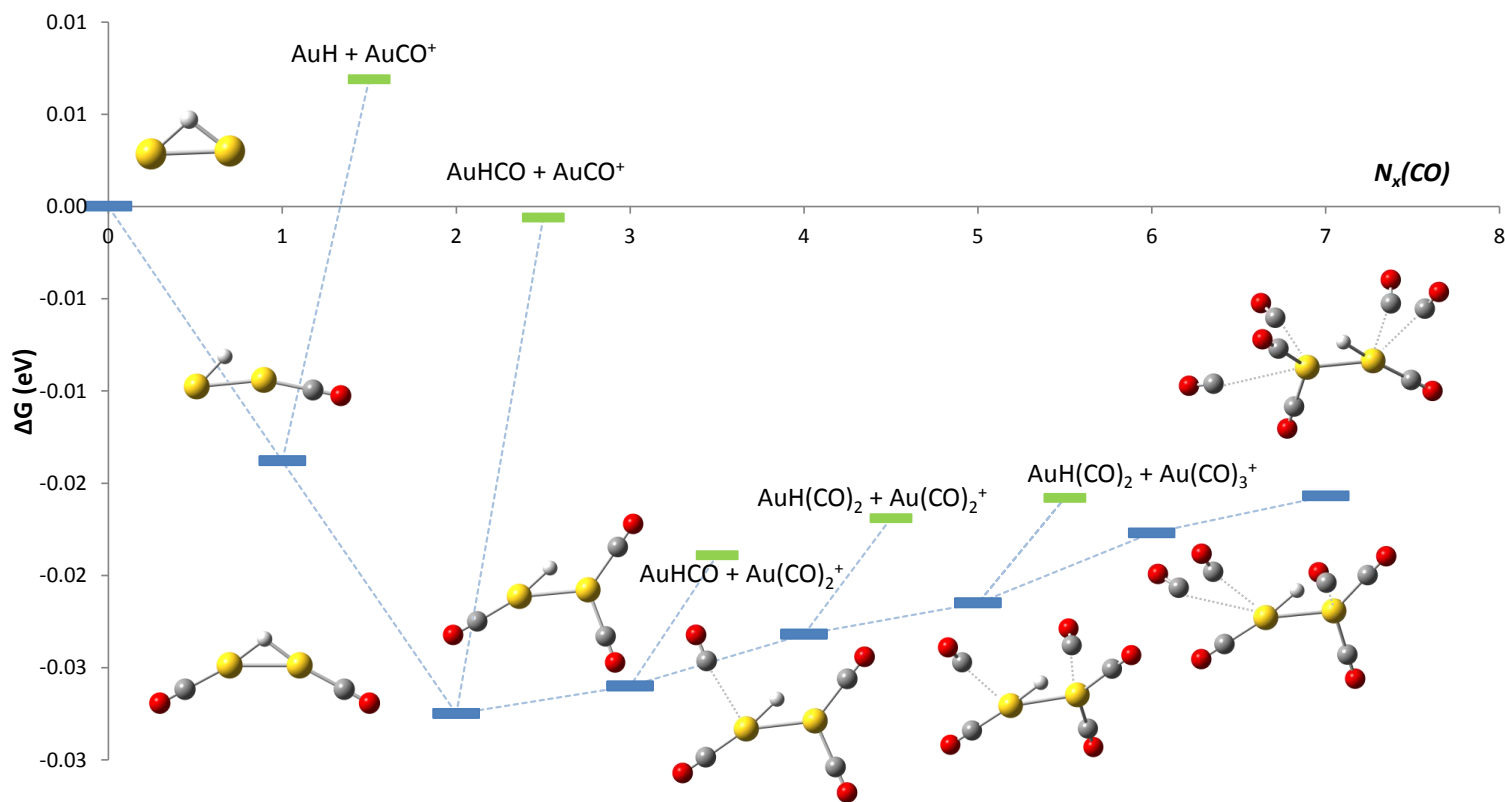


**Figure 5.** Free energy diagram (in eV) of the  $\text{Au}_2\text{H}^+$  complex as a function of the number of coordinating CO. The blue points correspond to coordinated complexes. Green points correspond to dissociated species. The free energies of the dissociated complexes:  $\text{AuH} + \text{AuCO}^+$ ,  $\text{AuHCO} + \text{AuCO}^+$ ,  $\text{AuHCO} + \text{Au}(\text{CO})_2^+$ ,  $\text{AuH}(\text{CO})_2 + \text{Au}(\text{CO})_2^+$  and  $\text{AuH}(\text{CO})_2 + \text{Au}(\text{CO})_3^+$  are  $\Delta G = +0.69$  eV,  $-0.06$  eV,  $-1.89$  eV,  $-1.69$  eV and  $-1.58$  eV, respectively.



## REFERENCES

1. Masatake, H.; Tetsuhiko, K.; Hiroshi, S.; Nobumasa, Y., Novel Gold Catalysts for the Oxidation of Carbon Monoxide at a Temperature Far Below 0 °C. *Chemistry Letters* **1987**, *16*, 405-408.
2. Haruta, M., Size- and Support-Dependency in the Catalysis of Gold. *Catalysis Today* **1997**, *36*, 153-166.
3. Hvolbæk, B.; Janssens, T. V. W.; Clausen, B. S.; Falsig, H.; Christensen, C. H.; Nørskov, J. K., Catalytic Activity of Au Nanoparticles. *Nano Today* **2007**, *2*, 14-18.
4. Spivey, J. J.; Editor, *Metal Nanoparticles for Catalysis : Advances and Applications* RSC: Cambridge, 2014.
5. Luo, Z.; Castleman, A. W.; Khanna, S. N., Reactivity of Metal Clusters. *Chem. Rev.* **2016**, *116*, 14456-14492.
6. Jordan, A. J.; Lalic, G.; Sadighi, J. P., Coinage Metal Hydrides: Synthesis, Characterization, and Reactivity. *Chemical Reviews* **2016**, *116*, 8318-8372.
7. Khairallah, G. N.; O'Hair, R. A. J., Gas Phase Synthesis and Reactivity of Ag<sup>n+</sup> and Ag<sup>n</sup>-1h<sup>+</sup> Cluster Cations. *Dalton Transactions* **2005**, 2702-2712.
8. Jena, N. K.; Chandrakumar, K. R. S.; Ghosh, S. K., Theoretical Investigation on the Structure and Electronic Properties of Hydrogen- and Alkali-Metal-Doped Gold Clusters and Their Interaction with Co: Enhanced Reactivity of Hydrogen-Doped Gold Clusters. *The Journal of Physical Chemistry C* **2009**, *113*, 17885-17892.
9. Buckart, S.; Ganteför, G.; Kim, Y. D.; Jena, P., Anomalous Behavior of Atomic Hydrogen Interacting with Gold Clusters. *J. Am. Chem. Soc.* **2003**, *125*, 14205-14209.
10. Bus, E.; van Bokhoven, J. A., Hydrogen Chemisorption on Supported Platinum, Gold, and Platinum Gold-Alloy Catalysts. *Phys. Chem. Chem. Phys.* **2007**, *9*, 2894-2902.
11. Fischer, D.; Andreoni, W.; Curioni, A.; Gronbeck, H.; Burkart, S.; Ganteför, G., Chemisorption on Small Clusters: Can Vertical Detachment Energy Measurements Provide Chemical Information? H on Au as a Case Study. *Chem. Phys. Lett.* **2002**, *361*, 389-396.
12. Ghosh, A.; Ghanty, T. K., Unprecedented Enhancement of Noble Gas-Noble Metal Bonding in NgAu<sup>3+</sup> (Ng = Ar, Kr, and Xe) Ion through Hydrogen Doping. *The Journal of Physical Chemistry A* **2016**, 9998–10006.
13. Mondal, K.; Agrawal, S.; Manna, D.; Banerjee, A.; Ghanty, T. K., Effect of Hydrogen Atom Doping on the Structure and Electronic Properties of 20-Atom Gold Cluster. *The Journal of Physical Chemistry C* **2016**, *120*, 18588-18594.
14. Phala, N. S.; Klatt, G.; Steen, E. v., A Dft Study of Hydrogen and Carbon Monoxide Chemisorption onto Small Gold Clusters. *Chemical Physics Letters* **2004**, *395*, 33-37.
15. Zhao, S.; Ren, Y.; Ren, Y.; Wang, J.; Yin, W., Density Functional Study of Hydrogen Binding on Gold and Silver–Gold Clusters. *The Journal of Physical Chemistry A* **2010**, *114*, 4917-4923.
16. Lang, S. M.; Bernhardt, T. M.; Barnett, R. N.; Yoon, B.; Landman, U., Hydrogen-Promoted Oxygen Activation by Free Gold Cluster Cations. *Journal of the American Chemical Society* **2009**, *131*, 8939-8951.
17. Jena, N. K.; Chandrakumar, K. R. S.; Ghosh, S. K., Beyond the Gold Hydrogen Analogy: Doping Gold Cluster with H-Atom O<sub>2</sub> Activation and Reduction of the Reaction Barrier for Co Oxidation. *J. Phys. Chem. Lett.* **2011**, *2*, 1476-1480.

18. Manzoor, D.; Pal, S., Reactivity and Catalytic Activity of Hydrogen Atom Chemisorbed Silver Clusters. *The Journal of Physical Chemistry A* **2015**, *119*, 6162-6170.
19. Ito, T.; Patwari, G. N.; Arakawa, M.; Terasaki, A., Water-Induced Adsorption of Carbon Monoxide and Oxygen on the Gold Dimer Cation. *The Journal of Physical Chemistry A* **2014**, *118*, 8293-8297.
20. Manzoor, D.; Pal, S., Hydrogen Atom Chemisorbed Gold Clusters as Highly Active Catalysts for Oxygen Activation and CO Oxidation. *The Journal of Physical Chemistry C* **2014**, *118*, 30057-30062.
21. Vojkovic, M.; Rayane, D.; Bertorelle, F.; Antoine, R.; Broyer, M.; Dugourd, P., Synthesis of Ligated-Metal Species by Laser Vaporization Electrospray Ionization (Lavesi). *International Journal of Mass Spectrometry* **2015**, *387*, 45-50.
22. O'Hair, R. A. J., The 3d Quadrupole Ion Trap Mass Spectrometer as a Complete Chemical Laboratory for Fundamental Gas-Phase Studies of Metal Mediated Chemistry. *Chemical Communications* **2006**, 1469-1481.
23. Becker, W., The Turbomolecular Pump, Its Design, Operation and Theory; Calculation of the Pumping Speed for Various Gases and Their Dependence on the Forepump. *Vacuum* **1966**, *16*, 625-632.
24. Berger, R. J. F., The Smallest "Auophilic Species". *Zeitschrift Fur Naturforschung Section B-a Journal of Chemical Sciences* **2009**, *64*, 388-394.
25. Grimme, S., Semiempirical Hybrid Density Functional with Perturbative Second-Order Correlation. *The Journal of Chemical Physics* **2006**, *124*, 034108.
26. Neese, F., The Orca Program System. *Wiley Interdisciplinary Reviews: Computational Molecular Science* **2012**, *2*, 73-78.
27. Frisch, M. J., et al. *Gaussian 09, Revision E.01*, Gaussian, Inc.: Wallingford, CT, USA, 2009.
28. Bernhardt, T. M., Gas-Phase Kinetics and Catalytic Reactions of Small Silver and Gold Clusters. *International Journal of Mass Spectrometry* **2005**, *243*, 1-29.